

1 Epidemiological, phylogenetic, and resistance heterogeneity among *Acinetobacter baumannii* in a major US

2 Deep South healthcare center

3

4 Emma Graffice<sup>a</sup>, Derek B. Moates<sup>bc</sup>, Sixto M. Leal Jr.<sup>bc</sup>, Megan Amerson-Brown<sup>bc</sup>, Juan J. Calix<sup>a#</sup>

5

6 <sup>a</sup>Department of Medicine, Division of Infectious Disease, University of Alabama at Birmingham, Birmingham,  
7 Alabama, USA

8 <sup>b</sup>Department of Pathology, Division of Laboratory Science, University of Alabama at Birmingham, Birmingham,  
9 Alabama, USA

10 <sup>c</sup>University of Alabama at Birmingham Hospital Clinical Microbiology, Birmingham, Alabama, USA

11

12 Running Head: Molecular epidemiological survey of *A. baumannii*

13

14 #Address correspondence to Juan J. Calix, [juancalix@uabmc.edu](mailto:juancalix@uabmc.edu).

15

16 Author contributions:

17 J.J.C. and E.G. conceptualized, designed and performed the study. S.M.L., D.B.M., and M.A.B contributed to  
18 design and completion of the study. E.G. wrote the manuscript first draft. All authors were involved with  
19 manuscript revisions and approved the final version.

20

1 **Abstract:**

2 *Acinetobacter baumannii* (*Ab*) disease in the U.S. is commonly attributed to outbreaks of one or two  
3 monophyletic carbapenem resistance (CR) *Ab* lineages that vary by region. However, there is limited  
4 knowledge regarding *Ab* epidemiology and population structure in the U.S. Deep South, and few studies  
5 compare contemporary CR and carbapenem-susceptible (Cs) *Ab*, despite prevalence of the latter. We  
6 performed a 12-year time series analysis of *Ab* cases in a large hospital in Birmingham, AL, and 89 isolates  
7 from an ongoing surveillance project started in November 2021 were analyzed by whole genome sequencing  
8 and antibiotic susceptibility testing (AST). Cumulative CR rate among 2462 cases since 2011 was 19.4%, with  
9 increased rates during winter months resulting from seasonal changes in Cs*Ab* incidence. Sequenced CR*Ab*  
10 belonged to clonal complex (CC) 1, CC108, CC250, CC2, and CC499. Most CR*Ab* CCs were comprised of  
11 isolates that clustered apart from U.S. counterparts in phylogenetic analysis, despite being identified in  
12 unrelated cases occurring  $\geq 3$  months apart. In contrast, 38/47 (81%) Cs*Ab* isolates each belonged to a distinct  
13 CC. CR*Ab* isolates displayed lineage-distinct AST features, including unique carbapenem resistance genetic  
14 determinants and presumptive heteroresistance behaviors unique to CC108 and CC499 isolates. This first  
15 comprehensive analysis of *Ab* cases in the U.S. Deep South revealed epidemiological trends consistent with  
16 those in other regions and an unusually high degree of phylogenetic diversity among regional CR*Ab* isolates.  
17 We also describe emergent U.S. CR*Ab* lineages whose unconventional antimicrobial resistance features must  
18 be integrated into ongoing diagnostic, treatment, and surveillance efforts.

## 23 Introduction

24 The looming global health threat posed by multidrug resistant (MDR) organisms is best exemplified by  
25 the ESKAPE pathogens: vancomycin-resistant *Enterococcus faecium*, methicillin-resistant *Staphylococcus*  
26 *aureus*, extended-spectrum beta-lactamase (ESBL)-producing *Klebsiella pneumoniae*, carbapenem-resistant  
27 (CR) *Acinetobacter baumannii* (*Ab*), multidrug-resistant *Pseudomonas aeruginosa*, and ESBL *Enterobacter*  
28 species<sup>1</sup>. CR*Ab* in particular is considered a top priority for research by the World Health Organization<sup>2</sup> and  
29 U.S. CDC<sup>3</sup>. This is due to its ability to survive in various environments and its various multidrug resistant  
30 (MDR) phenotypes mediated by intrinsic *Acinetobacter*-derived cephalosporinase (ADC) class C  $\beta$ -lactamases  
31 and OXA class D  $\beta$ -lactamases, polymorphisms in antibiotic targets, and a variety of other resistance genes --  
32 including extrinsic OXA and non-OXA carbapenamases -- acquired via mobile genetic elements (e.g.,  
33 plasmids, transposons, etc.). CR*Ab* disease is conventionally linked to hospital-acquired (HA) respiratory,  
34 endovascular, wound, and urinary infections mainly attributable to a subset of MDR global lineages within the  
35 otherwise genetically diverse species<sup>4-6</sup>.

36 *Ab* strains can be classified according to one of two multilocus sequence type (MLST) schemes<sup>7</sup>, and  
37 to avoid confusion, herein we exclusively use the Pasteur MLST scheme<sup>8</sup>. Single locus variant (SLV)  
38 sequence types (STs) can be further grouped into monophyletic lineages, or clonal clusters (CC), named  
39 according to the prevailing ST. CR*Ab*-associated lineages CC2, CC1 and CC79 comprised 61%, 5% and 3%,  
40 respectively, of the ~3500 genomes available on NCBI in early 2019<sup>9</sup>. U.S. clinical *Ab* populations have  
41 historically reflected global trends, with CC2 comprising 85% of CR*Ab* isolates in the first nationwide survey  
42 performed between 2008-2009<sup>10</sup> and 64% of isolates from CDC sentinel sites between 2013-2017<sup>11</sup>.  
43 In contrast, CC2 comprises <5% of sequenced isolates from Latin American countries<sup>9</sup>, demonstrating that  
44 regional population structures can vary significantly. Similarly, observations from U.S. single-center studies  
45 reveal wide variation over locations and time<sup>11-15</sup>. For example, most pre-2012 CR*Ab* isolates in a St. Louis,  
46 MO healthcare system were CC2 or CC79<sup>10</sup>, but local subclones of the unrelated ST406 (CC406) and ST499  
47 (CC499), the latter of which was first detected in Chicago in 2010<sup>16</sup>, rapidly became the most common CR*Ab*  
48 between 2017 and 2019<sup>13</sup>.

49 Awareness of *Ab* CCs propagating in a region could inform clinical practice, as recent evidence  
50 suggests that CR*Ab* lineages each display unique susceptibility patterns to non-carbapenem antibiotics and  
51 may differ in their epidemiological behavior<sup>13</sup>. Notably, little is known regarding the population structure of *Ab*  
52 in the US Deep South. Other than the inclusion of six Florida isolates<sup>10</sup>, published surveys have not included  
53 isolates from Deep South/Southeast region, where unique climate patterns and socioeconomic factors may  
54 selectively favor traits in this environmental microbe absent from pools in other regions. In addition, most  
55 recent surveys exclude cases associated with carbapenem-susceptible (Cs) *Ab*, despite these being a  
56 common cause of *Ab* disease and better representing the genetic diversity of the species. Indeed, 59.3% and  
57 22.0% of CR*Ab* isolates sequenced in the St. Louis study (n=59) belonged to ST499 and ST406 outbreaks,  
58 respectively, but each sequenced Cs*Ab* isolate (n=31) belonged to a distinct ST, reflecting a much more  
59 sporadic nature of Cs*Ab* infections<sup>13</sup>.

60 Here we report early findings from our investigation of *Ab* population dynamics in the U.S. Deep South.  
61 We compare the epidemiology of Cs*Ab* and CR*Ab* isolates identified over 12 years in a large healthcare  
62 system in Birmingham, Alabama and characterize the current population structure of clinically-relevant *Ab* by  
63 isolate whole genome sequencing (WGS). We report a link between emergent lineages and atypical  
64 antimicrobial resistance phenotypes, and contextualize findings within the greater population structure of *Ab*  
65 throughout the U.S.

66

## 67 **Methods**

68 **Study location and period.** This study was approved by the University of Alabama at Birmingham (UAB)  
69 Institutional Review Board (IRB# 30003572 and 30008212) and was performed in the UAB Healthcare system  
70 from July 1, 2010 to December 31, 2022. UAB is a large integrated inpatient and outpatient healthcare system  
71 serving Birmingham, Alabama, USA and surrounding areas. It employs Cerner electronic medical record  
72 (EMR) systems, which was queried using the Informatics for Integrating Biology and the Bedside (i2b2) tool  
73 hosted by the UAB Center for Clinical and Translation Science (CCTS). UAB Hospital and affiliated clinics use  
74 a central UAB Clinical Microbiology Laboratory (UAB-CML) housed on the main campus.

75

76 **Retrospective study design and definitions.** For all cases in which *Acinetobacter* isolates were identified via

77 standard of care culture, we retrieved patient demographics, culture tissue source, hospital day of culture (if  
78 applicable), and antibiotic susceptibility testing (AST) interpretation results. The species identity of bacterial  
79 isolates was determined by automated biochemical methods or matrix-assisted laser desorption/ionization and  
80 time-of-flight mass spectroscopy (MALDI-TOF MS) performed in the UAB-CML. Only the first isolate per  
81 patient (“index culture”) reported as following was eligible for inclusion: “*Acinetobacter baumannii*” (n=419),  
82 “*Acinetobacter baumannii* complex” (n=651), “*Acinetobacter baumannii* complex/*haemolyticus*” (n=5), or  
83 “*Acinetobacter baumannii/haemolyticus*” (n=1387). Per UAB-CML protocols, all *Acinetobacter* isolates are  
84 routinely tested for susceptibility via the Beckman Coulter Microscan WalkAway plus AST system. Common  
85 AST within the UAB-CML includes ampicillin-sulbactam (SAM), cefepime (FEP), ceftazidime (CAZ),  
86 ciprofloxacin (CIP), gentamycin (GM), levofloxacin (LVX), trimethoprim-sulfamethoxazole (SXT), tobramycin  
87 (TOB), imipenem (IPM), and meropenem (MEM). AST and susceptibility reporting is performed according to  
88 Clinical and Laboratory Standards Institute (CLSI) guidelines<sup>17</sup>.

89 Isolates non-susceptible to either imipenem or meropenem by minimum inhibitory concentration (MIC)-  
90 AST were defined as CR. Cases were classified into 5 anatomical categories according to isolate source:  
91 “respiratory,” “skin and soft tissue/musculoskeletal” (SST/MSK), “urinary,” “blood” (including isolates obtained  
92 from central lines, endovascular devices, or grafts), or “other.” Cases were defined as HA if the index culture  
93 was performed  $\geq 48$  hours from time of hospitalization and before discharge. All other isolates were defined as  
94 nHA. To evaluate for seasonal trends among cases identified in 2011-2022, cases were grouped into four  
95 quarters according to the month index culture was obtained: 1 (January-March), 2 (April-June), 3 (July-  
96 September) and 4 (October-December).

97  
98 **Prospective isolate banking.** Since November 2021, clinical isolates typed as an *Acinetobacter* species by  
99 MALDI-TOF MS in the UAB-CML were identified via biweekly query of the UAB Cerner EMR system and  
100 eligible for inclusion. Subclones from original culture plates were transferred to the research laboratory for  
101 processing. If more than one morphologically distinct colony on culture plate was identified  
102 as *Acinetobacter*, all colonies were stored. For this staging study, we arbitrarily chose 89 presumptive *Ab*

isolates identified between November 1, 2021 and November 31, 2022 for sequencing and susceptibility testing analysis (Data S1). Herein, study isolates are named by number (e.g., isolate 002 denotes UAB\_Ab002, etc.).

**Whole genome sequencing, assembly and comparative genomics.** A full description of the well-established processing pipelines<sup>13</sup> used for genome assembly and comparative genomics analyses is provided in the Supplementary Text. The earliest isolate with a MLST and/or antimicrobial resistance gene (ARG) profile per person was denoted as an index isolate, with subsequent isolates denoted as non-index isolates.

**Kirby-Bauer AST.** Study isolates were tested by Kirby-Bauer disk diffusion AST (KB-AST) in our research lab with Mueller-Hinton agar against sulbactam/ampicillin (SAM), cefepime (FEP), ceftazidime (CAZ), meropenem (MEM), imipenem (IPM), trimethoprim/sulfamethoxazole (SXT), ciprofloxacin (CIP), gentamicin (GM) and doxycycline (DOX). Zone of clearance (ZOC) breakpoints were determined and interpreted according to CLSI guidelines<sup>17</sup>. In cases where subpopulations of distinct colonies were repeatedly observed growing up to the border of the antibiotic disk but readily distinguishable from the lawn's major border, we subcloned bacteria from colonies at the disk border ("disk subclone") or from the main lawn ("lawn subclone"). Subclones were plated and incubated at 37°C for 16 hours on LB Miller agar without antibiotics and retested by KB-AST the next day. Plate images were acquired from a height of 6.3 inches using an iPhone 14 Pro Max with 1x lens and arranged using Adobe Illustrator<sup>18</sup>.

**Systematic review of *Ab* isolate population structure in the U.S.** Full description of the systematic literature review and comparative genomic meta-analysis is provided in the Supplementary Text. Briefly, a screen on NCBI database was performed on September 18, 2023 and identified 774 genome sequences of *Ab* isolates identified in U.S. populations since 2010 in peer-reviewed reports. We performed *de novo* genome assembly using NCBI SRA files and, when available, extracted epidemiological and microbiological metadata (Data S2). Genomes were binned into CCs according to MLST analysis, and comparative genomic analysis was done within each CC. In the case where a CC of interest was absent among identified genomes (i.e.,

130 CC108), we manually screened for genomes on NCBI whose metadata indicated they were isolated in the U.S.  
131 since 2010.

132

133 **Statistical analyses.** Univariate analyses were performed with SPSS v29 (IBM, USA) or RStudio software v  
134 4.1.2<sup>19</sup>. Chi-squared or odd ratio test were performed for comparing categorical variables. Mann-Whitney test  
135 with Bonferroni adjustment for multiple comparisons was performed for continuous variables. Statistical  
136 significance was defined as  $p$  value  $<0.05$ .

137

138 **Data availability.** All raw sequence files and assemblies derived from UAB study strains are available under  
139 NCBI BioProject PRJNA1005294 (see Data S1).

140

## 141 **Results**

142 **Retrospective analysis reveals diverse clinical presentations of *Ab* cases at UAB.** We identified 2462  
143 cases associated with *Ab* index cultures at UAB between July 2010 and December 2022, including 478  
144 (19.4%) cases with *CRAb* (Data S3). *CsAb* but not *CRAb* case occurrence displayed seasonality, with the  
145 selective increase in incidence of *Cs* cases during third calendar quarters (Figure 1A) resulting in decreased  
146 CR rates between May and October (Figure 1B). 41.6% (826/1984) of *CsAb* cases were HA, compared to  
147 54.2% (259/478) of *CRAb*. Though *CRAb* cases were more likely than *CsAb* to be HA (54.2% versus 41.6%,  
148 OR [CI95%]=1.66 [1.36-2.03]), HA rates fluctuated over time among *CRAb*. HA rates were 76.9% and 85.7%  
149 in late 2010 and early 2011, respectively, but were 27.4% and 45.5% in both halves of 2022 (Data S3). This  
150 trend coincided with *CRAb* cases in later periods being identified earlier during hospitalization (Figure 1C). In  
151 contrast, *CsAb* HA rates and median hospital day of isolation were similar in all study periods (Figure 1D).  
152 *CsAb* and *CRAb* displayed comparable distribution of isolate tissue sources when stratified according to onset  
153 (Figure 1E), i.e., respiratory isolates predominated among HA cases, while urinary and SST/MSK isolates  
154 predominated among nHA cases in nearly all study periods (Figure 1F). Lastly, *CRAb* was more likely to be  
155 isolated from males (OR [CI95%] = 1.49 [1.21-1.84]), and females comprised less than 40% of *CsAb*  
156 respiratory cases (37.2%) and *CRAb* respiratory (37.7%), SST/MSK (33.1%) urinary (34.7%), and other

(31.6%) cases (Table S1). There was no difference in average patient age between *CsAb* (49.0 years) and *CRAb* (50.3 years,  $p=0.178$ ) cases. In summary, *CRAb* and *CsAb* were both implicated in various case types at UAB, albeit with differential features regarding seasonality, timing of index culture, and patient sex distribution.

**2021-2022 UAB *Ab* isolates demonstrate phylogenetic heterogeneity.** To describe the *Ab* population structure in our cohort, we performed WGS of 89 *Ab* isolates identified in 2021-2022, including 73 index isolates from all tissue sources, obtained from 68 case patients (Figure 2, Data S1). We identified 31 assigned STs (including ST2139 and ST2140, which were newly assigned in this study) and 11 unassigned STs distributed among 39 CCs (Table S2). Ten cases had >1 *Ab* isolate included in our WGS analysis, and three patients had two index isolates from unrelated STs (Figure S1). 58.9% ( $n=43$ ) of index isolates belonged to nine CCs, each containing  $\geq 2$  index isolates obtained from unrelated cases occurring  $\geq 30$  days apart (Figure 2, Table S2). Of these, CC108, CC164 and CC427 each contained isolates of two STs. The remaining index isolates ( $n=30$ ) each belonged to unrelated STs (Data S4).

**Antimicrobial susceptibility was linked to lineage dependent and independent genetic elements.** We investigated whether UAB *CRAb* lineages display distinctive AST profiles, as observed in recent studies<sup>13</sup>. Our cohort was comprised of 26 *CRAb* and 47 *CsAb* index isolates (Figure 3, Data S1). CC108 and CC499 were exclusively comprised of *CRAb*, CC150, CC164, CC32 and CC427 were comprised exclusively of *CsAb*, and CC1, CC2 and CC250 were comprised of both. All remaining isolates were *CsAb*. ARG analysis revealed all CC499 isolates encode OXA-24, the CC108 isolate 260 encodes OXA-499 (an OXA-143-like carbapenemase), and OXA-23 is encoded in nearly all other CR isolates except isolate 032 (Figure 3). Along with six other CC108 isolates, isolate 032 encodes the FtsI A515V polymorphism, a penicillin-binding protein 3 mutation predicted to decrease carbapenem binding to its active site<sup>20</sup>. In summary, carbapenem resistance wholly correlated with the presence of attributable genetic elements (Figure 3, Data S4).

The identity of intrinsic OXA and ADC alleles was largely conserved within a lineage and rarely shared between lineages (Figure 3). Independent of OXA-23 presence, CC1 and CC2 isolates displayed greater FEP



184 and CAZ resistance than other *CsAb*, including the CC250 *CsAb* isolates (Figure S2). Conversely, CC250 and  
185 CC499 *CRAb* isolates displayed CAZ susceptibility indistinguishable from CC150 and other *CsAb*. CC108  
186 isolates displayed the lowest detectable levels of susceptibility across all beta-lactam antibiotics in KB-AST  
187 (Figure S2). We observed comparably greater intra-CC variation in the susceptibility to other antibiotic classes,  
188 which strongly correlated with the presence of resistance elements repeatedly shared by genomes in multiple  
189 lineages (Figure 3 and Figure S2). The only major discrepancy was SXT non-susceptibility in CC499 isolate  
190 who lacked the *sul1/sul2* gene putatively conferring resistance in all other lineages, which is a trait observed  
191 among CC499 isolates in prior studies<sup>13</sup>.

192  
193 **Atypical resistance phenotypes displayed by CC108 and CC499 isolates.** Results from clinical laboratory  
194 AST by microbroth dilution (MB-AST) generally matched Kirby-Bauer AST (KB-AST) for most isolates, but two  
195 consistent discrepancies were noted (Data S1, S5). First, CC108 isolates displaying the lowest detectable  
196 susceptibility to SAM in KB-AST were reported as “intermediate” or “susceptible” according to MB-AST.  
197 Second, despite CC499 isolates being reported as “susceptible” to SXT according to MB-AST and lacking  
198 conventional resistance gene elements observed in other SXT-resistant isolates, they displayed decreased  
199 susceptibility to SXT in KB-AST. Closer review of KB-AST plates found that CC108 isolates against IPM and  
200 SAM and CC499 isolates against SXT each displayed subpopulations extending between their main lawn  
201 margin and the antibiotic disk borders (Figure 4A). Subclones obtained from the lawn or colonies at the  
202 antibiotic disk border were incubated overnight without antibiotics, and secondary KB-AST was performed  
203 (Figure 4B). Each subclone pair yielded similar results in secondary KB-AST (Figure 4C-E). Similar SXT-  
204 related phenomenon was observed when testing ST499 isolates identified prior to 2019 in St. Louis (Figure  
205 S3)<sup>13</sup>. No other tested isolates displayed similar patterns in KB-AST.

206  
207 **Meta-analysis of contemporary U.S. *Ab* population structures.** The equal presence of multiple unrelated  
208 *CRAb* lineages in our cohort was unexpected. To understand how strains in our cohort relate to their lineages  
209 in the greater U.S. *Ab* population, we integrated 645 *Ab* genomes from strains isolated in U.S. since 2010 that  
210 passed QC (Data S2) and 545 genomes were used for CC-specific comparative analyses (Table S2). UAB

211 CC2 isolates occupied three branches within two previously described clades<sup>14,21</sup>, one branch in Clade C  
212 (isolates 021 and 187) and two in Clade A (isolate 028 and all the others, respectively) (Figure 5). Most CC1,  
213 CC499, CC108 and CC250 UAB isolates occupied exclusive branches within their complexes, though two  
214 CC250 (isolates 024 and 232) and CC108 isolates (isolates 076 and 260) were on distinct branches.  
215 Conversely, UAB CC150 and CC32 genomes were broadly distributed within their respective trees. No CC427  
216 or CC164 isolates were identified in the U.S. meta-analysis, and two of the most common U.S. lineages,  
217 CC406 (also known as USA-clone-1<sup>22</sup>) and CC79 (also known as Clade E<sup>14</sup>), were absent from the UAB cohort  
218 (Table S2).

219 In ARG analysis of the total U.S. cohort there was within-lineage variability regarding strains harboring  
220 resistance genetic elements for non-beta-lactam antibiotics (Data S2). In contrast, the allelic identity of intrinsic  
221 OXA and ADC genes facilitated the delineation of phylogenetic subclades within clonal complexes, most of  
222 which included isolates obtained in different studies and regions (Figure S4). The vast majority of isolates  
223 encoding a carbapenemase contained OXA-23. However, OXA-24/72 was the prevalent carbapenemase  
224 among CC2 isolates in subclades A2, C2 and G (Figure S4B), half of CC79 isolates, two unrelated subclades  
225 in CC406, and nearly all non-Mountain region CC499 isolates (Figure S4C). Notably, the FtsI A515V  
226 polymorphism was encoded by isolates only in CC2 subclade B2 (Figure S4B) and one CC108 subclade that  
227 included isolates lacking any OXA carbapenemase (Figure S4C). CC406 was the only CRAb-associated  
228 complex in which most isolates had no identifiable carbapenem resistance element. CC150 and CC32 isolates  
229 did not encode carbapenemases (Figure S4D).

## 231 Discussion

232 We report a comprehensive analysis of clinical cases associated with *Ab* isolates in a major Deep  
233 South U.S. medical center. Aiming to uncover the microbiological landscape of *Ab* propagating in our region,  
234 we followed an ecological study design to characterize the presentation of *Ab*-associated cases and the  
235 population structure of clinical isolates. Investigation of treatment strategies, outcomes, and transmission  
236 networks spurring their presence is the subject of ongoing study in our regional cohort.

237 Few recent surveys include both *CsAb* and *CRAb* in their analyses despite the former being more  
238 prevalent among *Ab* clinical isolates in many regions<sup>6,23</sup>. *CRAb* cases were more likely to be HA in our cohort,  
239 though the trend of cases being identified earlier in a hospital course did not coincide with a decrease in  
240 carbapenem resistance (Data S3), and tissue source distributions of CS and CR isolates were  
241 indistinguishable (Figure 1E-F). The observed link between tissue source distribution and case onset as well  
242 as the presence of seasonality only among *CsAb* (Figure 1A-B) is consistent with prior reports<sup>6,24</sup>. Altogether,  
243 these findings support that our cohort is comparable to *Ab* in other U.S. medical centers.

244 Genomic analysis identified multiple clusters comprised of isolates collected  $\geq 90$  days apart, from  
245 different tissue sources, and associated with HA and nHA cases (Figure 2), and many of these isolates belong  
246 to subclades unique to our region. Attributing *Ab* clusters to hyperlocalized outbreaks would require a formal  
247 clonality analysis beyond the scope of our current study. Regardless, these observations imply the existence of  
248 contemporary microbial pools persisting in the region and outside our hospital, as shown in other U.S.  
249 regions<sup>13,14</sup>. While 26 index *CRAb* belonged to five CCs, 47 *CsAb* isolates belonged to 37 unrelated lineages.  
250 The identification of multiple cases in a single U.S. center caused by single lineages (i.e. CC150 and CC32)  
251 has not been reported. However, compared to *CRAb* isolates, there tended to be greater distance between  
252 UAB *CsAb* isolates within their respective CCs (Figure 5). The relatively decreased relatedness among *CsAb*  
253 isolates is consistent with recent reports<sup>13</sup>, and support that *CsAb* cases are result of sporadic cross-over  
254 events from environmental sources.

255 As a species living in undefined environmental niches, *Ab* harbors a very diverse genetic pool even  
256 compared to other Gram-negative pathogens<sup>25,26</sup>. Though historically most *CRAb* disease has been attributed  
257 to CC2 isolates, unrelated lineages have recently emerged in the U.S. For example, the first reported  
258 incidence of ST499 isolation occurred in 2010<sup>16</sup>, but CC499 has now become the second most common  
259 lineage among U.S. *CRAb* isolates and the dominant lineage in some regions<sup>11,13</sup>. CC108 had been only  
260 sporadically observed in prior studies, but our finding support it is capable of establishing a stable presence in  
261 a region. Lastly, ST250 was first identified in a 2007 isolate from Puerto Rico<sup>27</sup>, rarely identified in prior U.S.  
262 surveillance, but repeatedly isolated from unrelated cases over the course of our study. As reflected by the  
263 relative diversity of *CRAb* lineages concurrently propagating in our region, climate in the U.S. Deep South may

264 be more permissive to *Ab* phylogenetic diversity than other sites where surveillance has previously been  
265 performed<sup>11</sup>, and we predict similarly diverse *Ab* population structures would be revealed upon investigation of  
266 other Deep South sites. These findings highlight that we should avoid generalizing historical or even  
267 multicenter study findings to local *Ab* population structures, as the lineages responsible for local cases can  
268 differ drastically from site to site.

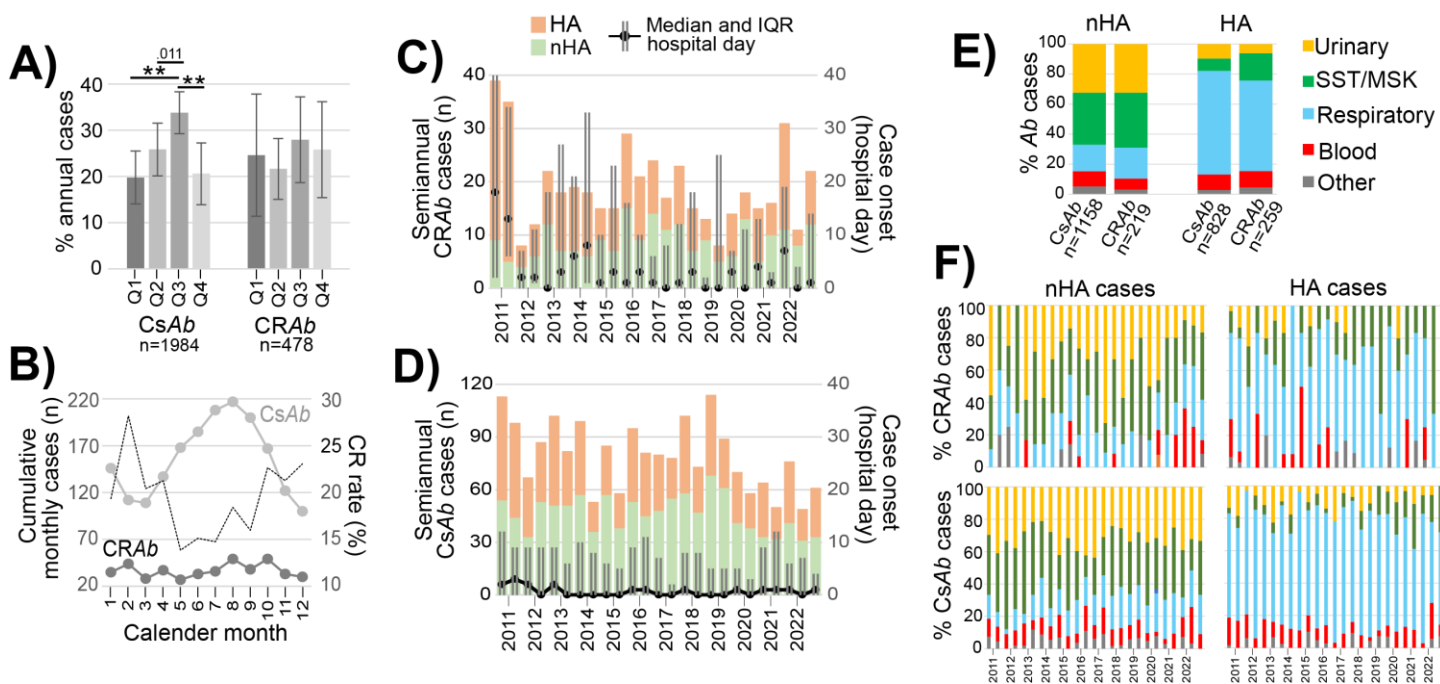
269 The value of surveilling local population structures remains to be determined, as the contribution of *Ab*  
270 phylogeny to pathogenesis and clinical outcomes is unclear. However, consistent with prior findings<sup>28</sup>, we  
271 observed that CR*Ab* lineages can harbor unique antimicrobial resistance features that may influence local  
272 medical practices. For example, OXA-23 has historically been the most prevalent carbapenamase among  
273 CR*Ab* and, thus, is a target of current and emergent rapid molecular detection tools in clinical labs<sup>29</sup>. However,  
274 we identified U.S. isolates belonging to CC2, CC108, and CC499 that display carbapenem resistance via other  
275 resistance determinants (i.e., OXA-24 or the FtsI A515V polymorphism), and the mechanism of carbapenem  
276 resistance among CC406 isolates remains to be identified<sup>13,22</sup> (Figure S4). During the preparation of this  
277 manuscript, Sabour, et al. reported that carbapenemase gene content among CR*Ab* differed by region, and  
278 these genes did not appear to always confer the same degree of resistance<sup>28</sup>. Though Sabour et al. did not  
279 evaluate whether degree of carbapenem resistance was dependent on lineage, lineage-associated differences  
280 were observed previously<sup>13</sup> and in our study (i.e., OXA-23-associated IPM resistance was greater among CC2  
281 isolates compared to CC250 isolates, Figure S2). Altogether, this implies that the utility of OXA-23-based  
282 testing varies according to which U.S. lineages are circulating in the region.

283 Another concerning finding was the discordance between MB-AST and KB-AST for SAM against  
284 CC108 isolates and for SXT against CC499 isolates. The repeated occurrence of subpopulations with different  
285 susceptibilities and the instability of increased resistance phenotype in subclones together suggest the  
286 presence of heteroresistance in these isolates, though further work is required to confirm and characterize this.  
287 Why these traits are not readily identifiable via MB-AST, and how the spontaneous occurrence of increased  
288 resistance against sulbactam and trimethoprim/sulfamethoxazole influences clinical outcomes or susceptibility  
289 to new combination agents (i.e., sulbactam-durlobactam), must be evaluated. The dynamic nature of these  
290 resistance phenotypes is reminiscent of phase variation, but the mechanisms through which the phenotype is

291 achieved require further study. This is especially true for CC499, which appears able to achieve elevated  
292 resistance to SXT without harboring any of the genetic elements typically associated with SXT resistance in  
293 other *Ab* lineages (i.e. *sul1* or *sul2*, Figure 3).

294        Though consistent with recent reports from other U.S. locations<sup>11-13</sup>, our study was performed in a  
295 single healthcare center and the generalizability of findings to other global *Ab* populations remains to be  
296 determined. Importantly, our work begins to show how knowledge of isolate lineage could influence clinical  
297 decision-making and sets a foundation to explore how lineage may influence other aspects of *Ab* disease, such  
298 as virulence, clinical prognosis, and propensity to be spread among certain patient populations.

306



307

308 **Figure 1. Divergent epidemiological features of Ab cases at UAB, July 2010-December 2022.** A)

309 Proportion of annual carbapenem-susceptible *A. baumannii* (CsAb) and carbapenem-resistant Ab (CRAb)

310 cases occurring in each calendar quarter (Q1-Q4) during 2011-2022. \*\*, <0.001. B) Cumulative case total for

311 each month (left y-axis) of CsAb and CRAb (light and dark gray, respectively) and monthly CR rate (dotted line,

312 right y-axis) among cases from 2011-2022. C,D) Semiannual totals (left y-axis) of hospital-acquired (HA) and

313 non-hospital acquired (nHA) CRAb (panel C) and CsAb (panel D) cases. Lines and error bars depict the

314 median and interquartile range (IQR) for hospital day of isolation among cases in each period (right y-axis).

315 Panel C key corresponds to both panels. E) Percentage of CRAb and CsAb index isolate from each tissue

316 sources among nHA (left) and HA (right) cases. F) Percentage of index isolates from each source among CR

317 (top row) and Cs (bottom row) cases in each study period, separated by nHA (left column) and HA (right

318 column).

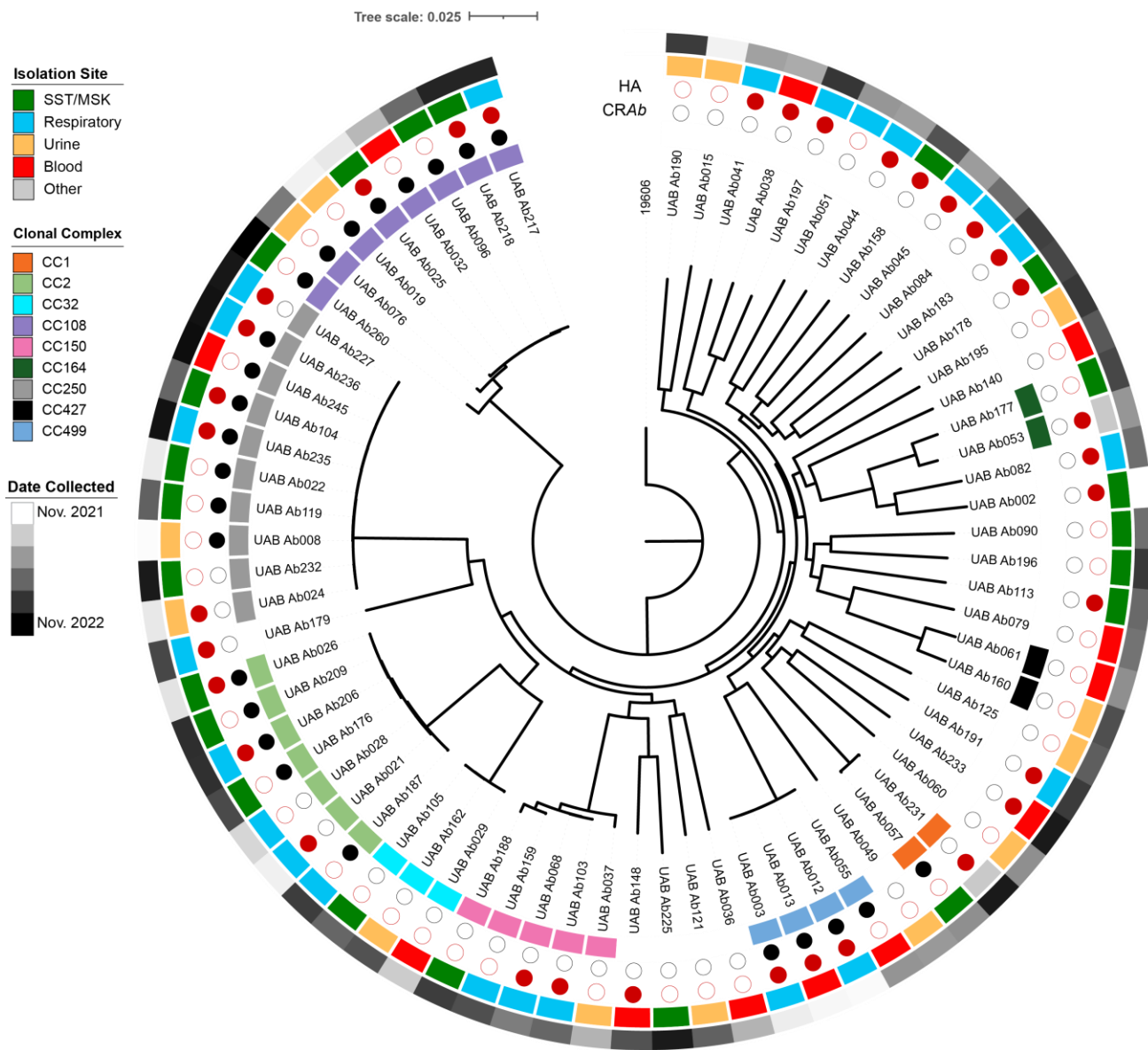


**Figure 2: Diversity of Ab isolates at UAB hospitals, 2021-2022.** Maximum likelihood phylogenetic tree of UAB Ab index isolates according to alignment of 2072 core genes, rooted to the genome of reference strains 19606. Inner label ring denotes CC with >1 index isolate. Filled circles denote CRAb and isolates associated with HA cases. Outer rings represent isolate metadata according to the corresponding keys, as listed in Data S1.

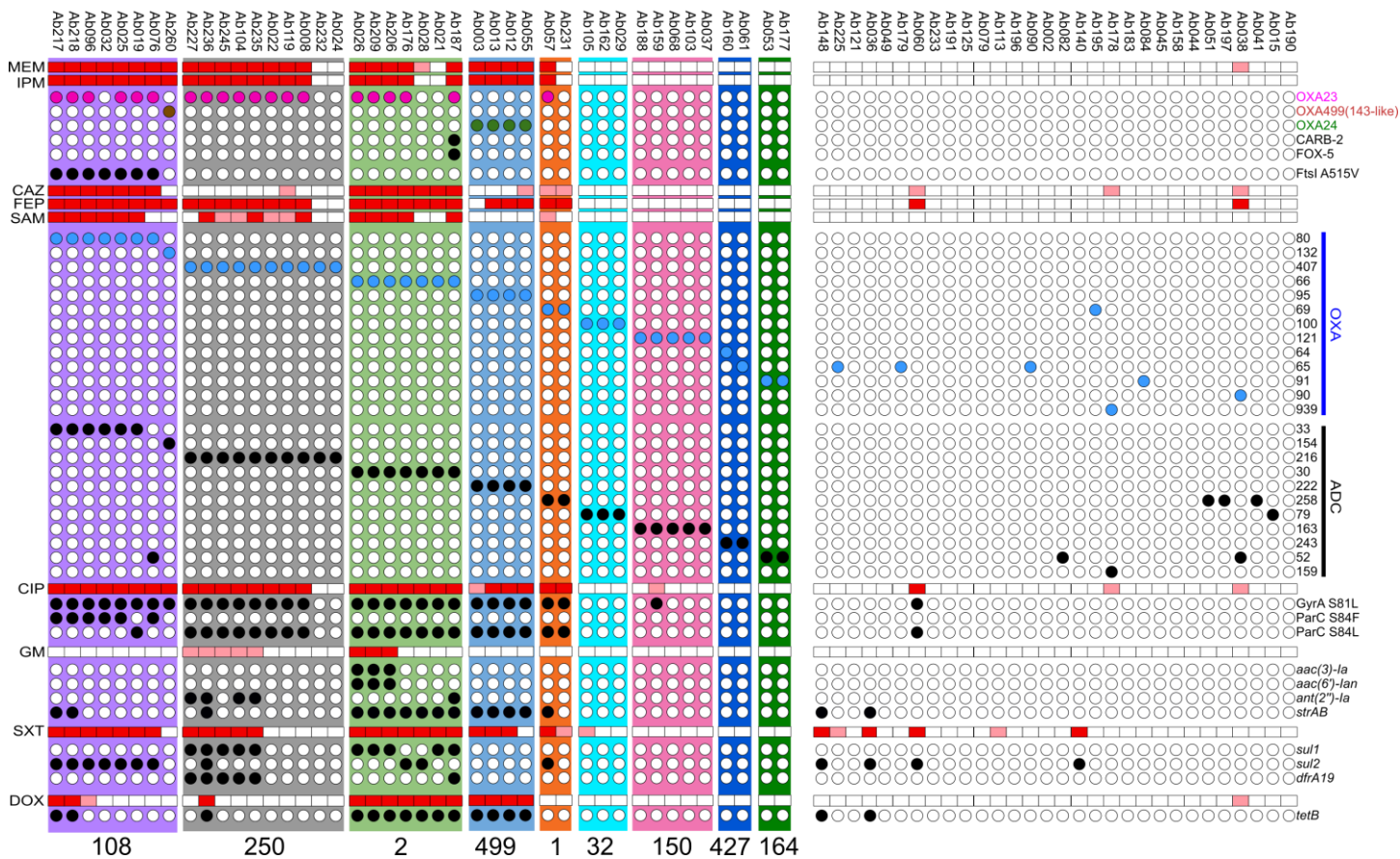


**Figure 3: Antibiotic susceptibility and resistance genetic element content of UAB index isolates (top).**

Tested antibiotics are listed on left and grouped by antibiotic class. Results are presented as “resistant” (red), “intermediate” (pink), or “susceptible” (white) according to CLSI guideline interpretation of Kirby-Bauer results.

Circles below each AST group denotes presence (fill circle) or absence of associated resistance genetic elements listed on right. Intrinsic OXA and ADC alleles are listed by allele number. For clarity, only genetic elements present in isolates belonging to multi-isolate CCs (colored columns with labels below) are included.

Results for all UAB isolates and genetic elements are listed in Data S4.



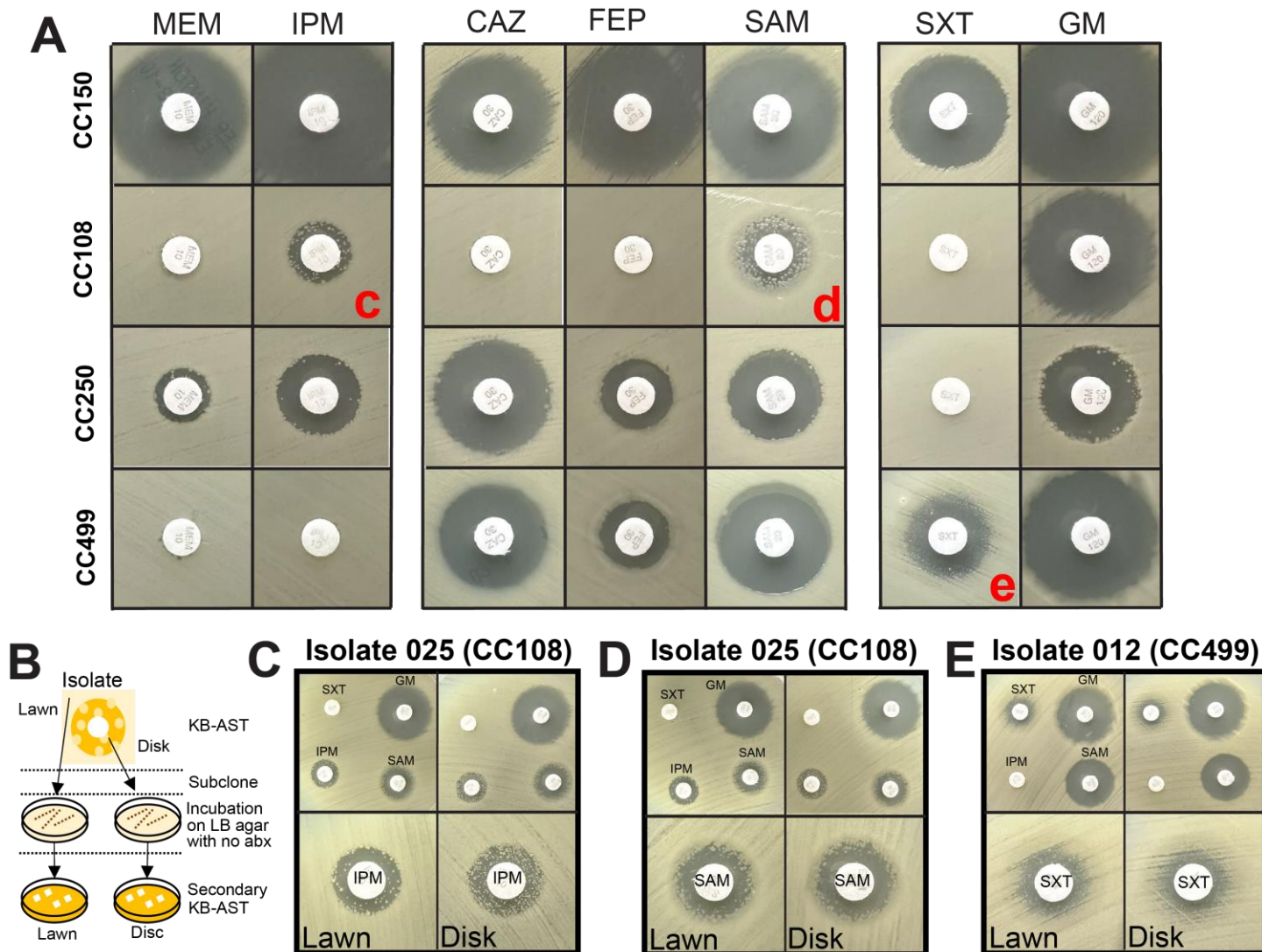


**Figure 4: KB-AST identifies susceptibility-variable subpopulations associated with CRAb lineage and**

**antibiotic type.** A) Representative pictures of the most commonly observed KB-AST results for main CCs in our cohort (left), against different antibiotics (top). Red letters denote samples that were subcloned and incubated overnight on LB agar with no antibiotic followed by secondary KB-AST, as depicted in panel B. C-E) Secondary KB-AST of “lawn” (left) and “disk” (right) subclones. Photos show results from multiple antibiotics (top) and magnification of zones of clearance around antibiotics of interest (bottom). MEM, meropenem; IPM, imipenem; CAZ, ceftazidime; FEP, cefepime; SAM, ampicillin-sulbactam; SXT, trimethoprim/sulfamethoxazole; GM, gentamicin.

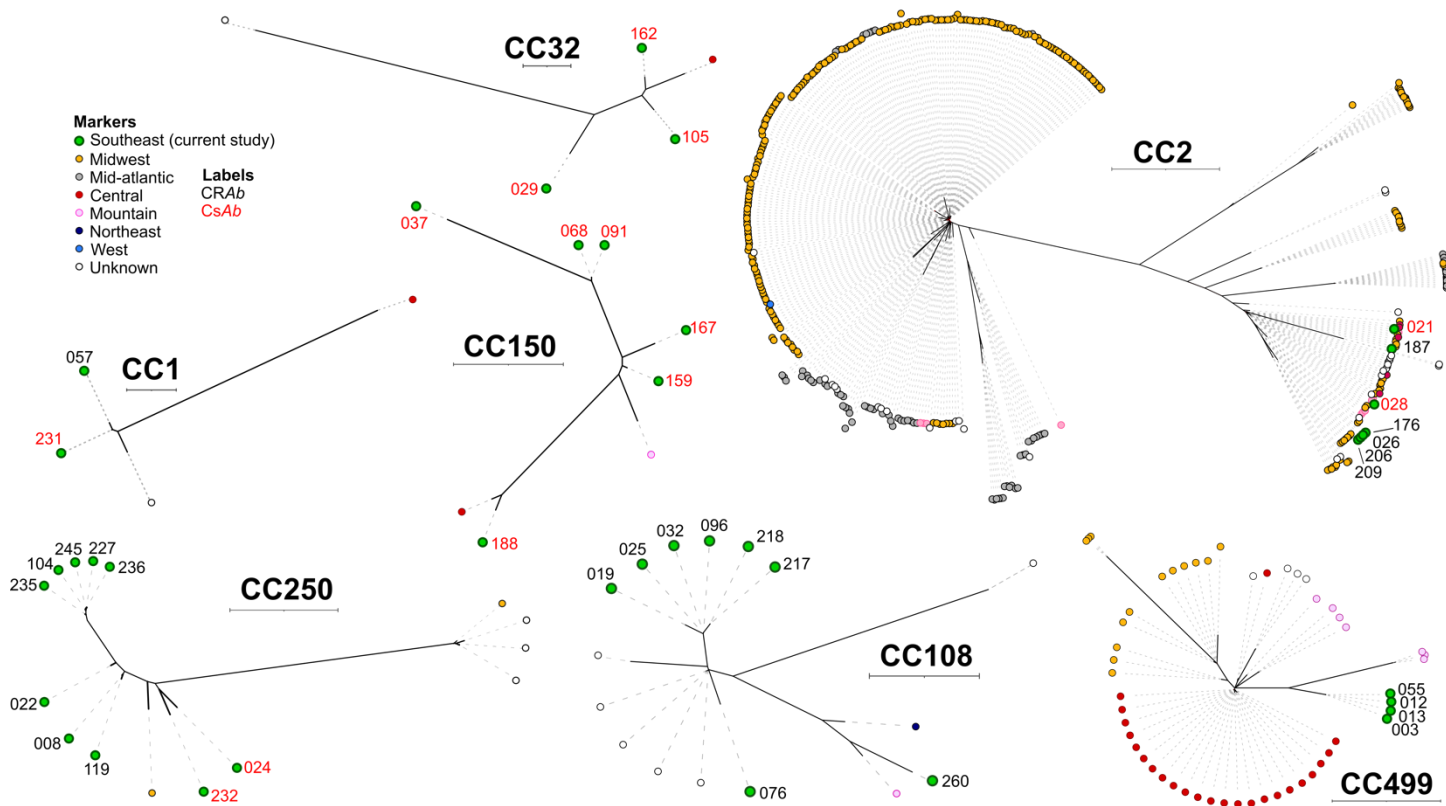
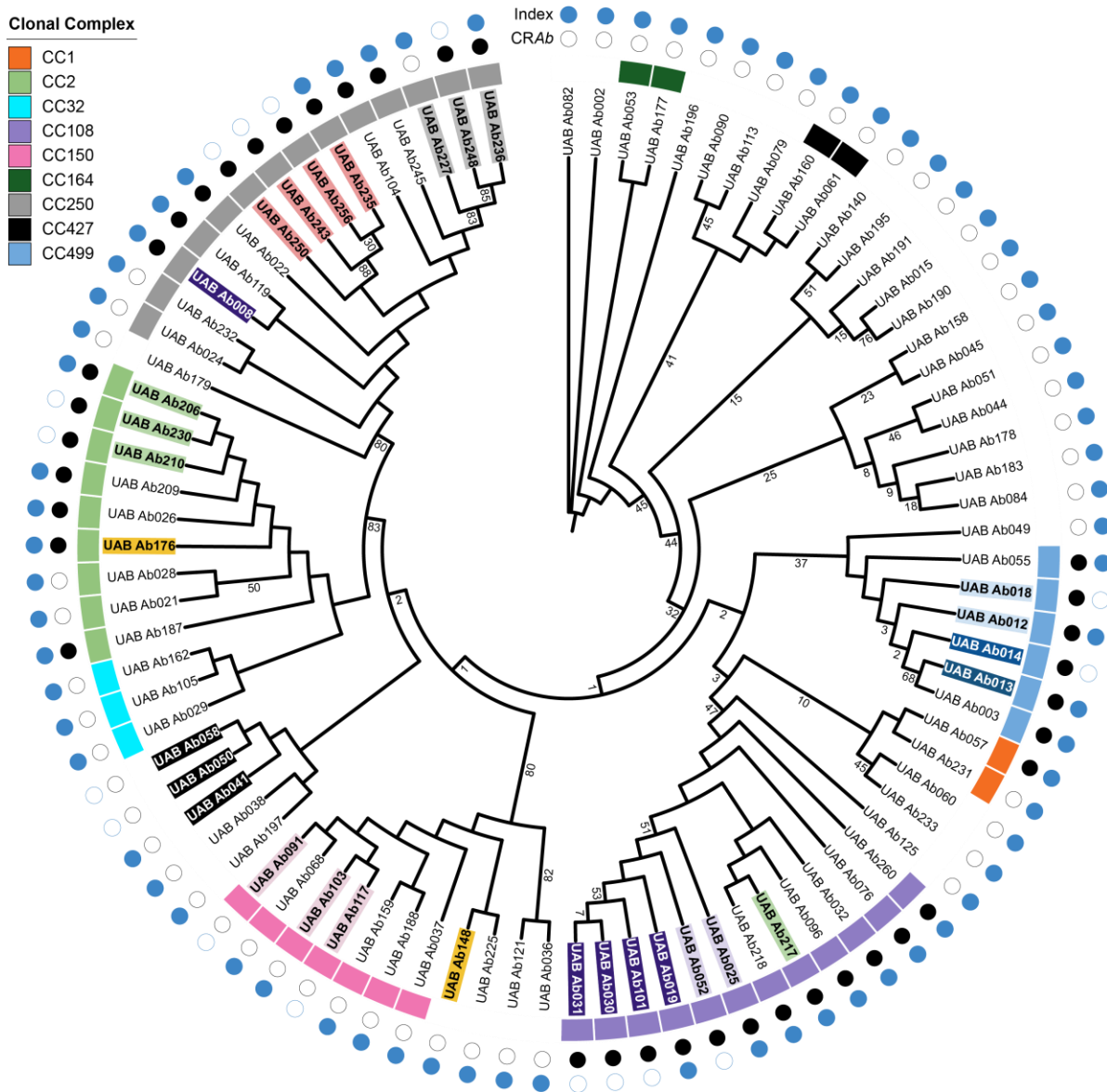


**Figure 5: Intra-CC phylogeny of U.S. *Ab* populations identified since 2010.** Unrooted maximum likelihood phylogenetic trees drawn according to alignment of core genes shared by isolates within each CC. Tree scales located under CC labels represent to 0.001 substitutions per site, with CC1 and CC32 trees presented as half scale compared to others. Leaf markers represent the regions where each isolate was identified, per the inset key. Numbered labels denote study number of carbapenem-resistant (black) or -susceptible (red) isolates in the UAB study.

356



357

358

**Figure S1: Phylogenetic clusters among all Ab sequenced isolates in this study.** Maximum likelihood tree

359

of all UAB Ab isolates, rooted to midpoint. Branches with bootstrap values <90% are labeled. Highlighted and

360

bolded leaves represent isolates obtained from the same patient, matched according to color. Outer boxes are

361

color coded according to key to denote CCs containing >1 index isolate. Carbapenem resistance and index

362

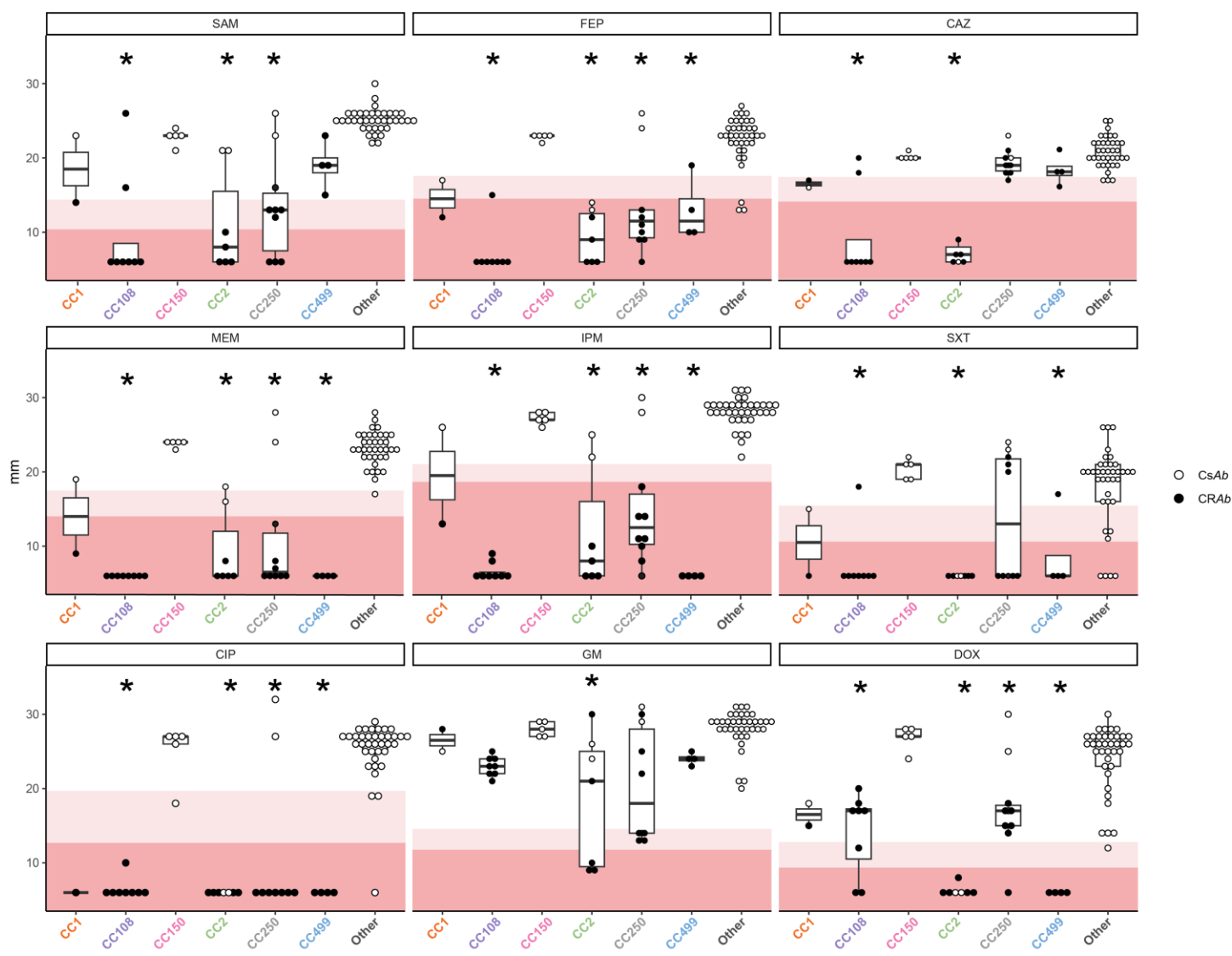
isolates are denoted by filled black and blue circles, respectively.

363

364

365

366



367

368

**Figure S2: Kirby-Bauer antimicrobial susceptibility testing (KB-AST) of UAB isolates.** Antibiotic

369

susceptibility, according to zone of clearance (mm, y-axis), of CRAb (black dots) and CsAb (white dots) index

370

isolates grouped by CC. Backgrounds highlight ranges for “resistant” (dark) and “intermediate” (light)

371

susceptibility, per CLSI guideline interpretation. Box-plot center lines denote medians; box limits, upper and

372

lower quartile values and whiskers, 1.5 times the IQR. Medians were compared to CC150 using Mann-Whitney

373

test with Bonferroni adjustment for multiple comparisons, with asterisks denoting  $P < 0.05$ . Abbreviations: CAZ,

374

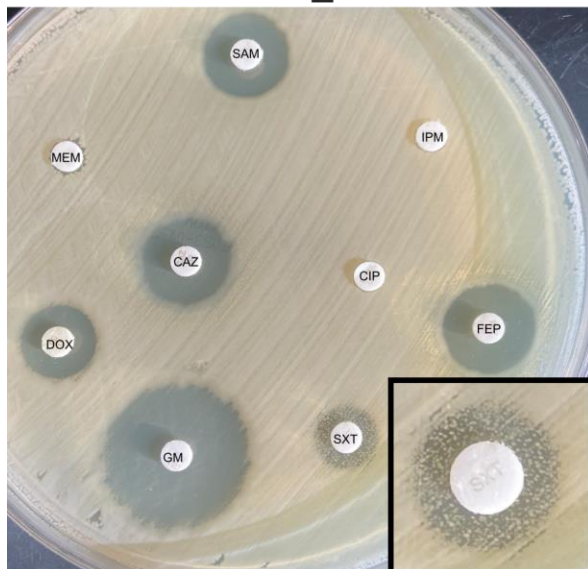
ceftazidime; CIP, ciprofloxacin; DOX, doxycycline; FEP, cefepime; GM, gentamicin; IPM, imipenem; MEM,

375

meropenem; SAM, ampicillin-sulbactam; SXT, trimethoprim-sulfamethaxazole.

376

## Isolate WU\_Ab164



377

378

**Figure S3: CC499 isolates from an unrelated cohort also display variable SXT susceptibility.** Photos of

379

KB-AST results of CC499 isolate WU\_Ab164, against of all tested antibiotics and magnification of zone of

380

clearance around SXT disk (inset). Abbreviations: CAZ, ceftazidime; CIP, ciprofloxacin; DOX, doxycycline;

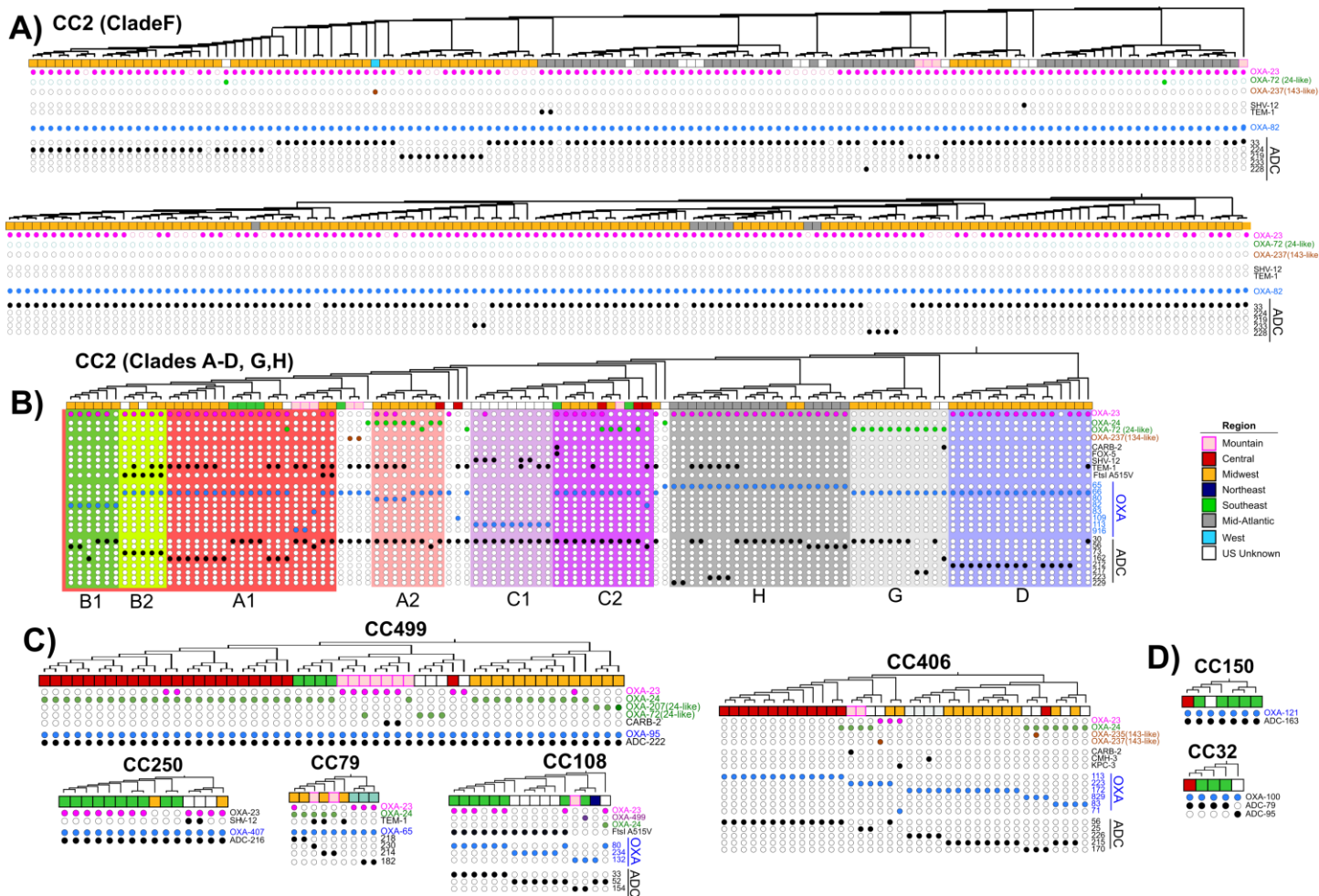
381

FEP, cefepime; GM, gentamicin; IPM, imipenem; MEM, meropenem; SAM, ampicillin-sulbactam; SXT,

382

trimethoprim-sulfamethaxazole.

383



384

385

386

387

388

389

390

391

**Figure S4: CC-wide ARG content among major U.S. lineages associated with CRAb (panels A-C) and CSAb (panel D).** Squares denote an isolate's region with color key in panel B. Top rows of matrices in panels A-C show OXA carbapenamases (labels colored according to subclass), followed by non-OXA genetic elements conferring  $\beta$ -lactam resistance in black. The lower lines denote intrinsic OXA (blue) and ADC (black) lactamase alleles. All genomes contain an ADC allele, but ADC alleles that were detected in only one genome are omitted for clarity.

392 **Table S1: Distribution of patient sex among UAB *Ab* cases.**

	Carbapenem susceptible <i>A. baumannii</i> specimen type						Carbapenem resistant <i>A. baumannii</i> specimen type					
	Blood	Other	Respiratory	SST/MSK	Urine	Total	Blood	Other	Respiratory	SST/MSK	Urine	Total
Male	110	39	483	241	231	1104	19	13	130	85	65	311
Female	91	45	292	228	224	880	25	6	71	42	22	166
% female	45.3%	53.6%	37.7%	48.6%	49.2%	44.4%	56.8%	31.6%	35.3%	33.1%	25.3%	34.7%
Sum	201	84	775	469	455	1984	44	19	201	127	87	478

393 SST/MSK, skin, soft tissue and musculoskeletal

394

395 **Table S2: Intra-lineage phenotypic and genotypic breakdowns.**

Clonal complex	UAB Cohort											U.S. Cohort (NCBI)								
	Days collected	Pasteur MLST	Index isolates	n CRAb (%)	nHA (%)	Tissue sources (n)					Genomic analysis				Genomes analyzed	Pasteur MLST	Total genes	Core genes	Core genome SNPs	SNPs/core gene
						SST/MSK	Urine	Resp.	Blood	Other	Total genes	Core genes	Core genome SNPs	SNP/core gene						
CC1	167	734	2	1 (50)	1 (50)	2	0	0	0	0	2792	3497	489	0.1398	4	1, 734	4210	3250	19806	6.0942
CC2	257	2	7	5 (71)	4 (57)	2	0	5	0	0	4570	3183	1650	0.5184	398	2, 195, 632, 1573	31307	2411	25625	10.6284
CC32	175	32	3	0 (0)	0 (0)	1	1	0	1	0	3933	3275	1878	0.5734	5	32	4343	3190	3231	1.0129
CC108	340	108, 2140	8	8 (100)	5 (63)	3	2	2	1	0	3861	3213	3339	1.0392	16	108, 2140	4550	2600	15102	5.8085
CC150	167	150	5	0 (0)	3 (60)	2	1	2	0	0	4152	3360	14860	4.4226	7	150	4458	3265	14325	4.3874
CC164	109	164, 1131	2	0 (0)	1 (50)	1	0	0	0	1	3857	3231	11631	3.5998	NA	NA	NA	NA	NA	NA
CC250	344	250	12	10 (83)	5 (42)	4	2	5	1	0	4819	3334	709	0.2127	15	250	4645	3140	1463	0.4659
CC427	89	427, 848	2	0 (0)	0 (0)	0	1	0	1	0	4261	3094	15695	5.0727	NA	NA	NA	NA	NA	NA
CC499	126	2139	4	4 (100)	1 (25)	0	0	2	2	0	3722	3677	26	0.0071	53	499, 1180, 2139	5034	3065	12489	4.0747
CC406	NA	NA	NA	NA	NA	NA	NA	NA	NA	NA	NA	NA	NA	NA	38	406, 1088, 1091, 1562	6248	2641	24797	9.3892
CC79	NA	NA	NA	NA	NA	NA	NA	NA	NA	NA	NA	NA	NA	NA	9	79	4639	3106	7655	2.4646

396 NA indicates where an analysis could not be performed.

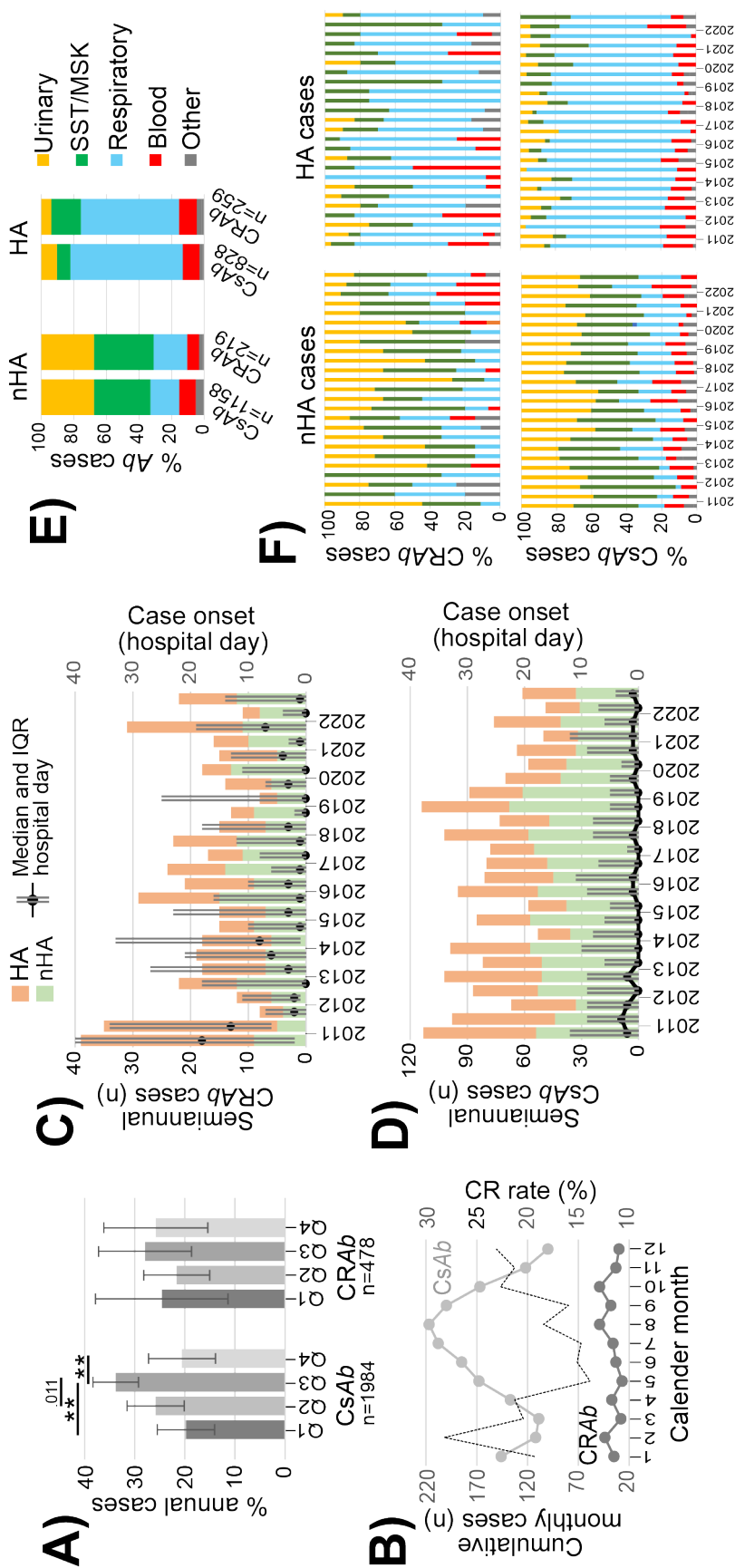
397

398 References:

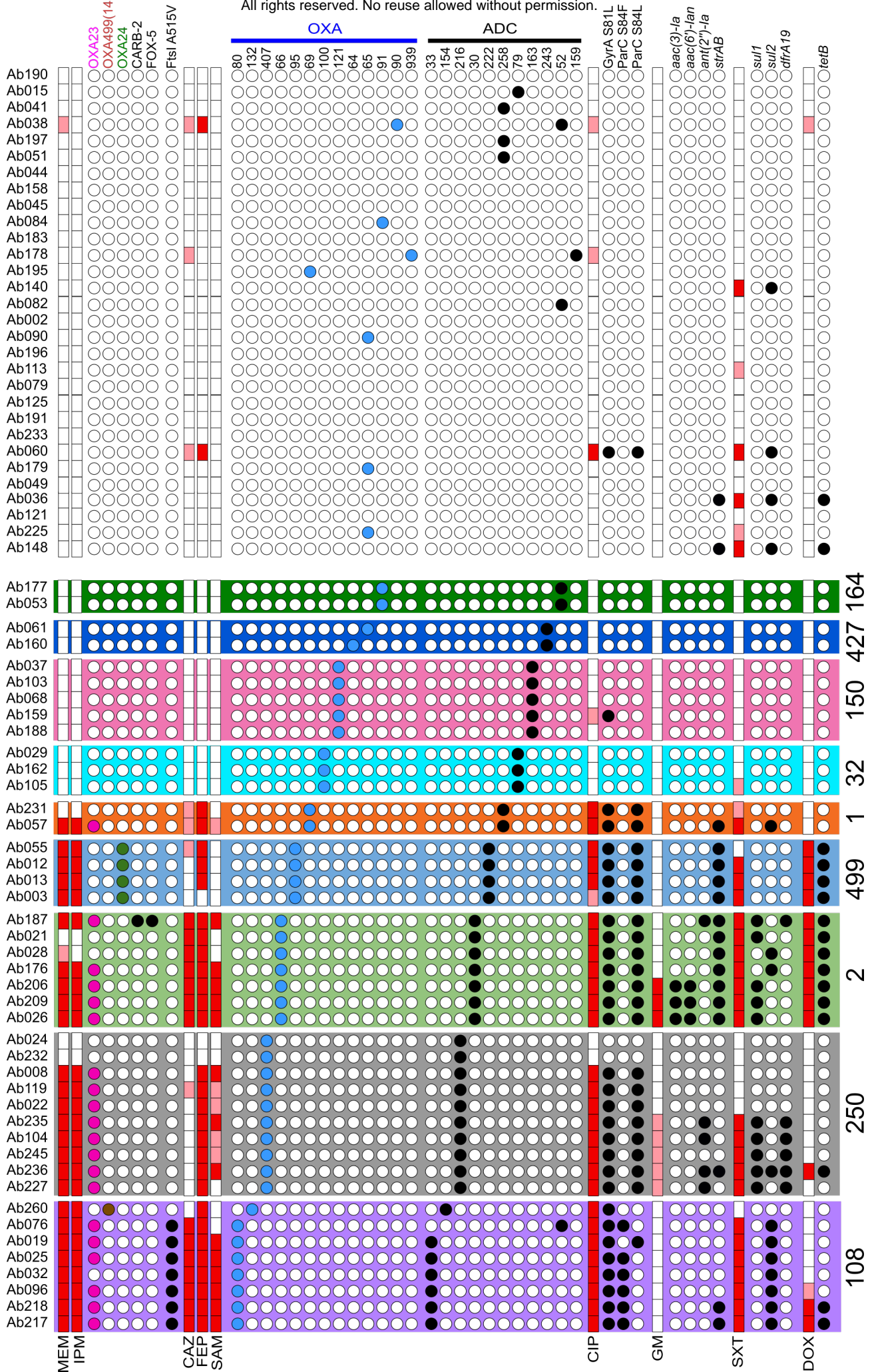
- 399 1 Rice, L. B. Federal funding for the study of antimicrobial resistance in nosocomial pathogens: no  
400 ESKAPE. *J Infect Dis* **197**, 1079-1081 (2008). <https://doi.org/10.1086/533452>
- 401 2 Tacconelli, E. *et al.* Discovery, research, and development of new antibiotics: the WHO priority list of  
402 antibiotic-resistant bacteria and tuberculosis. *Lancet Infect Dis* **18**, 318-327 (2018).  
403 [https://doi.org/10.1016/S1473-3099\(17\)30753-3](https://doi.org/10.1016/S1473-3099(17)30753-3)
- 404 3 CDC. Antibiotic Resistance Threats in the United States, 2019. *U.S. Department of Health and Human  
405 Services, CDC* (2019). <https://doi.org/http://dx.doi.org/10.15620/cdc:82532>.
- 406 4 Wong, D. *et al.* Clinical and Pathophysiological Overview of Acinetobacter Infections: a Century of  
407 Challenges. *Clin Microbiol Rev* **30**, 409-447 (2017). <https://doi.org/10.1128/CMR.00058-16>
- 408 5 Di Venanzio, G. *et al.* Urinary tract colonization is enhanced by a plasmid that regulates uropathogenic  
409 Acinetobacter baumannii chromosomal genes. *Nat Commun* **10**, 2763 (2019).  
410 <https://doi.org/10.1038/s41467-019-10706-y>
- 411 6 Calix, J. J., Burnham, J. P. & Feldman, M. F. Comparison of the Clinical Characteristics of Hospital-  
412 Acquired and Non-Hospital-Acquired Acinetobacter calcoaceticus-baumannii Complex in a Large  
413 Midwest US Health Care System. *Open Forum Infect Dis* **6**, ofz423 (2019).  
414 <https://doi.org/10.1093/ofid/ofz423>
- 415 7 Gaiarsa, S. *et al.* Comparative Analysis of the Two Acinetobacter baumannii Multilocus Sequence  
416 Typing (MLST) Schemes. *Front Microbiol* **10**, 930 (2019). <https://doi.org/10.3389/fmicb.2019.00930>
- 417 8 Jolley, K. A., Bray, J. E. & Maiden, M. C. J. Open-access bacterial population genomics: BIGSdb  
418 software, the PubMLST.org website and their applications. *Wellcome Open Res* **3**, 124 (2018).  
419 <https://doi.org/10.12688/wellcomeopenres.14826.1>
- 420 9 Hamidian, M. & Nigro, S. J. Emergence, molecular mechanisms and global spread of carbapenem-  
421 resistant Acinetobacter baumannii. *Microb Genom* **5** (2019). <https://doi.org/10.1099/mgen.0.000306>
- 422 10 Adams-Haduch, J. M. *et al.* Molecular epidemiology of carbapenem-nonsusceptible Acinetobacter  
423 baumannii in the United States. *J Clin Microbiol* **49**, 3849-3854 (2011).  
424 <https://doi.org/10.1128/JCM.00619-11>
- 425 11 McKay, S. L. *et al.* Molecular Epidemiology of Carbapenem-Resistant Acinetobacter baumannii in the  
426 United States, 2013-2017. *Microb Drug Resist* **28**, 645-653 (2022).  
427 <https://doi.org/10.1089/mdr.2021.0352>
- 428 12 Iovleva, A. *et al.* Carbapenem-Resistant Acinetobacter baumannii in U.S. Hospitals: Diversification of  
429 Circulating Lineages and Antimicrobial Resistance. *mBio* **13**, e0275921 (2022).  
430 <https://doi.org/10.1128/mbio.02759-21>
- 431 13 Calix, J. J. *et al.* Outpatient clonal propagation propelled rapid regional establishment of an emergent  
432 carbapenem-resistant Acinetobacter baumannii lineage ST499Pas. *J Infect Dis* (2022).  
433 <https://doi.org/10.1093/infdis/jiac427>
- 434 14 Adams, M. D. *et al.* Rapid Replacement of Acinetobacter baumannii Strains Accompanied by Changes  
435 in Lipooligosaccharide Loci and Resistance Gene Repertoire. *mBio* **10** (2019).  
436 <https://doi.org/10.1128/mBio.00356-19>
- 437 15 Fitzpatrick, M. A., Ozer, E. A. & Hauser, A. R. Utility of Whole-Genome Sequencing in Characterizing  
438 Acinetobacter Epidemiology and Analyzing Hospital Outbreaks. *J Clin Microbiol* **54**, 593-612 (2016).  
439 <https://doi.org/10.1128/JCM.01818-15>
- 440 16 Ozer, E. A., Fitzpatrick, M. A. & Hauser, A. R. Draft Genome Sequence of Acinetobacter baumannii  
441 Strain ABBL099, a Multidrug-Resistant Clinical Outbreak Isolate with a Novel Multilocus Sequence  
442 Type. *Genome Announc* **2** (2014). <https://doi.org/10.1128/genomeA.00738-14>
- 443 17 (Clinical and Laboratory Standards Institute, Wayne, PA, 2007).
- 444 18 Adobe Illustrator (2019).
- 445 19 Team, R. C. R: A Language and Environment for Statistical Computing. *R Foundation for Statistical  
446 Computing, Vienna, Austria* (2020).
- 447 20 Hawkey, J. *et al.* Evolution of carbapenem resistance in Acinetobacter baumannii during a prolonged  
448 infection. *Microb Genom* **4** (2018). <https://doi.org/10.1099/mgen.0.000165>

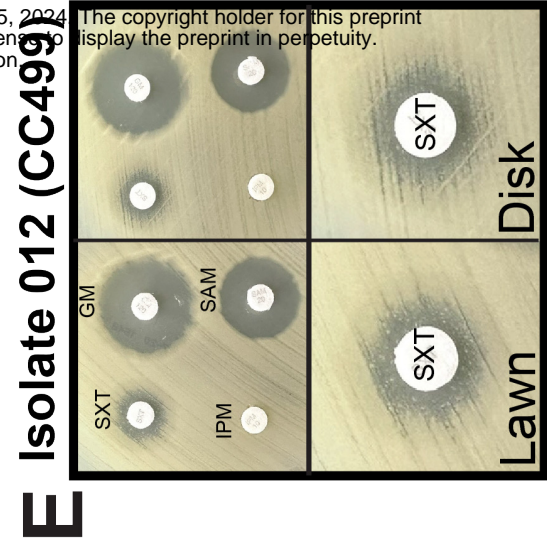
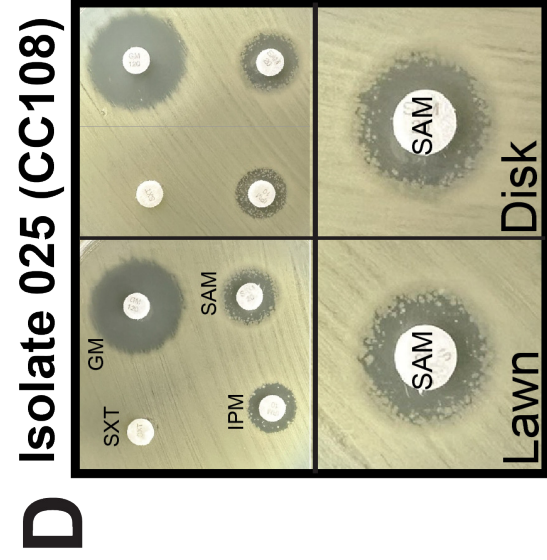
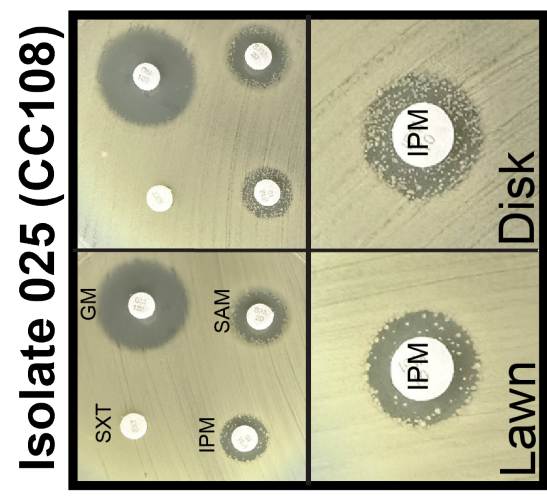
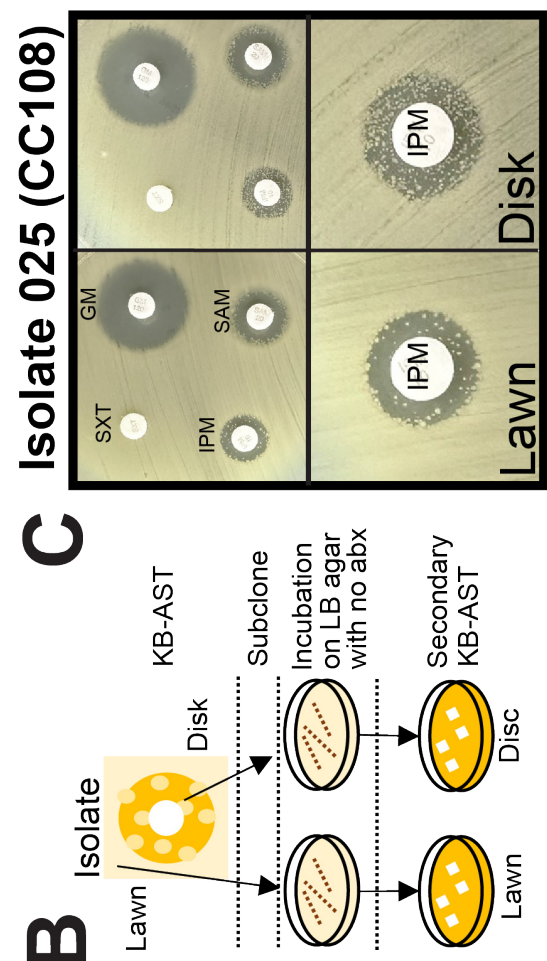
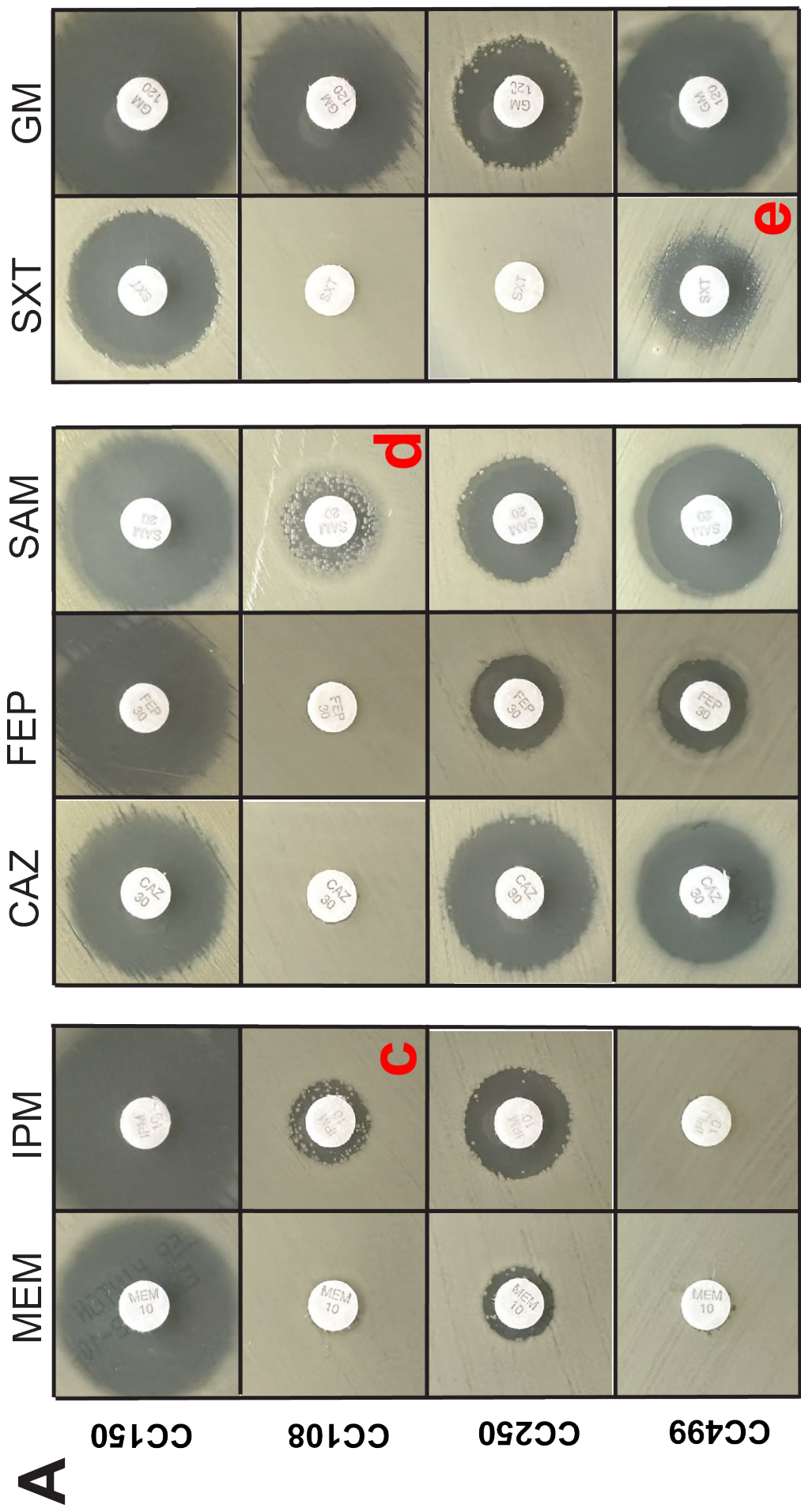


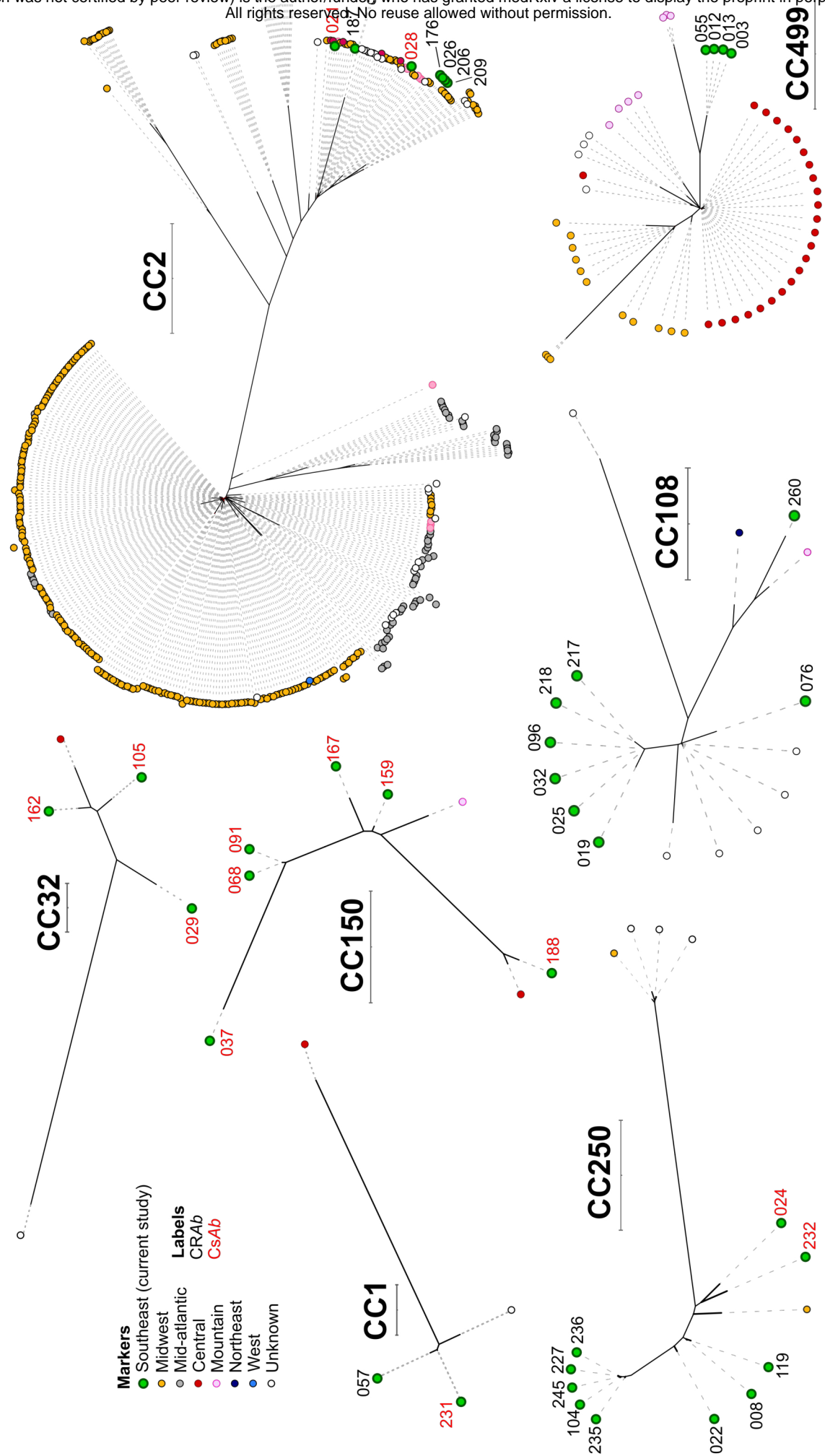
- 449 21 Wright, M. S. *et al.* New insights into dissemination and variation of the health care-associated  
450 pathogen *Acinetobacter baumannii* from genomic analysis. *MBio* **5**, e00963-00913 (2014).  
451 <https://doi.org/10.1128/mBio.00963-13>
- 452 22 Muller, C. *et al.* A global view on carbapenem-resistant *Acinetobacter baumannii*. *mBio* **14**, e0226023  
453 (2023). <https://doi.org/10.1128/mbio.02260-23>
- 454 23 Gales, A. C. *et al.* Antimicrobial Susceptibility of *Acinetobacter calcoaceticus*-*Acinetobacter baumannii*  
455 Complex and *Stenotrophomonas maltophilia* Clinical Isolates: Results From the SENTRY Antimicrobial  
456 Surveillance Program (1997-2016). *Open Forum Infect Dis* **6**, S34-S46 (2019).  
457 <https://doi.org/10.1093/ofid/ofy293>
- 458 24 Burnham, J. P., Feldman, M. F. & Calix, J. J. Seasonal Changes in the Prevalence of Antibiotic-  
459 Susceptible *Acinetobacter calcoaceticus*-*baumannii* Complex Isolates Result in Increased Multidrug  
460 Resistance Rates During Winter Months. *Open Forum Infect Dis* **6**, ofz245 (2019).  
461 <https://doi.org/10.1093/ofid/ofz245>
- 462 25 Chan, A. P. *et al.* A novel method of consensus pan-chromosome assembly and large-scale  
463 comparative analysis reveal the highly flexible pan-genome of *Acinetobacter baumannii*. *Genome Biol*  
464 **16**, 143 (2015). <https://doi.org/10.1186/s13059-015-0701-6>
- 465 26 Park, S. C., Lee, K., Kim, Y. O., Won, S. & Chun, J. Large-Scale Genomics Reveals the Genetic  
466 Characteristics of Seven Species and Importance of Phylogenetic Distance for Estimating Pan-Genome  
467 Size. *Front Microbiol* **10**, 834 (2019). <https://doi.org/10.3389/fmicb.2019.00834>
- 468 27 Martinez, T., Ropelewski, A. J., Gonzalez-Mendez, R., Vazquez, G. J. & Robledo, I. E. Draft Genome  
469 Sequence of *Klebsiella pneumoniae* Carbapenemase-Producing *Acinetobacter baumannii* Strain  
470 M3AC9-7, Isolated from Puerto Rico. *Genome Announc* **3** (2015).  
471 <https://doi.org/10.1128/genomeA.00274-15>
- 472 28 Sabour, S. *et al.* Descriptive analysis of targeted carbapenemase genes and antibiotic susceptibility  
473 profiles among carbapenem-resistant *Acinetobacter baumannii* tested in the Antimicrobial  
474 Resistance Laboratory Network, United States, 2017-2020. *Microbiology Spectrum* **12**,  
475 e02828-02823 (2024). <https://doi.org/10.1128/spectrum.02828-23>
- 476 29 Vasilakopoulou, A. *et al.* A multicentre evaluation of the NG-test DetecTool OXA-23 for the rapid  
477 detection of OXA-23 carbapenemase directly from blood cultures. *JAC Antimicrob Resist* **6**, dlae029  
478 (2024). <https://doi.org/10.1093/jacamr/dlae029>

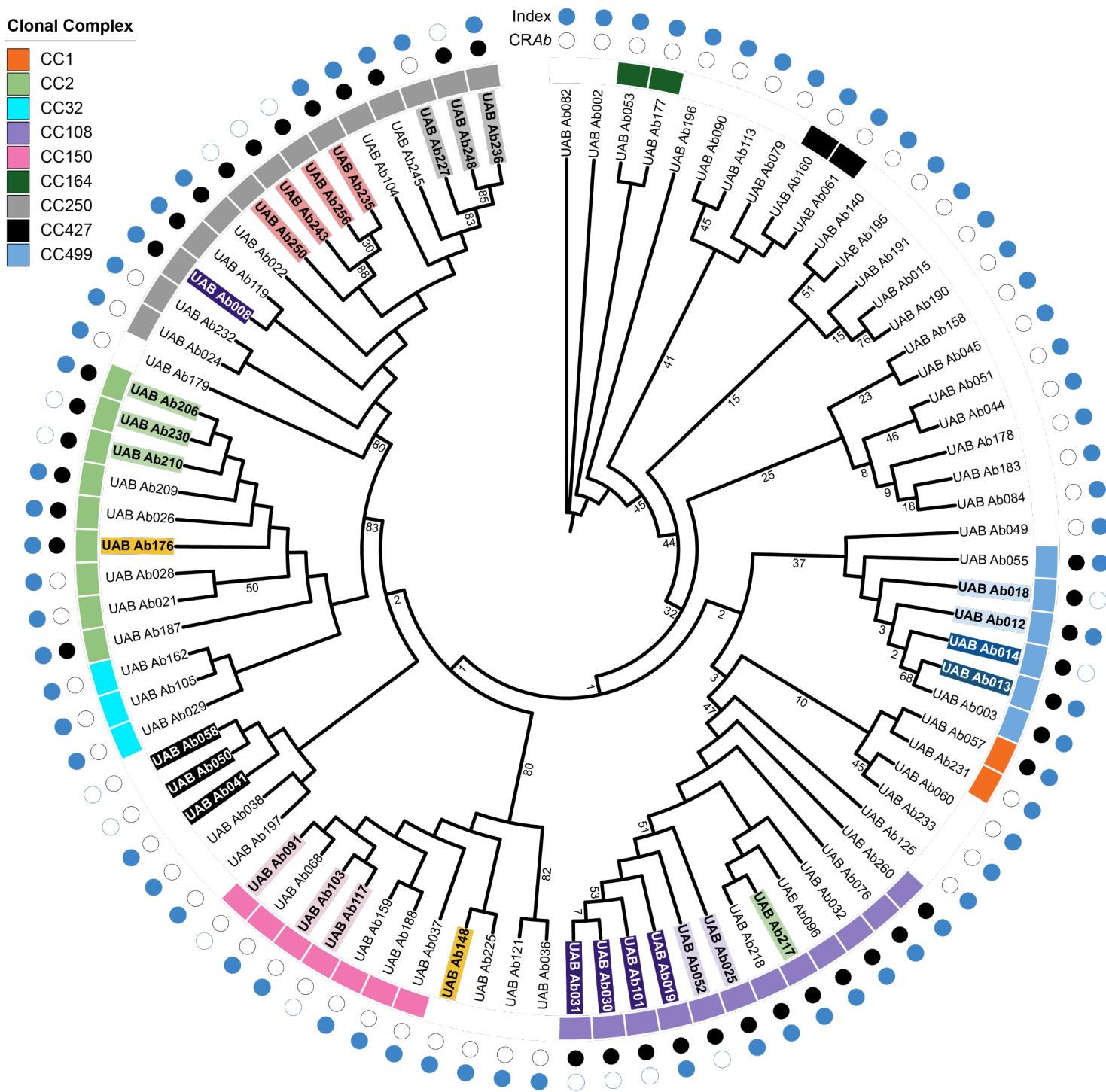




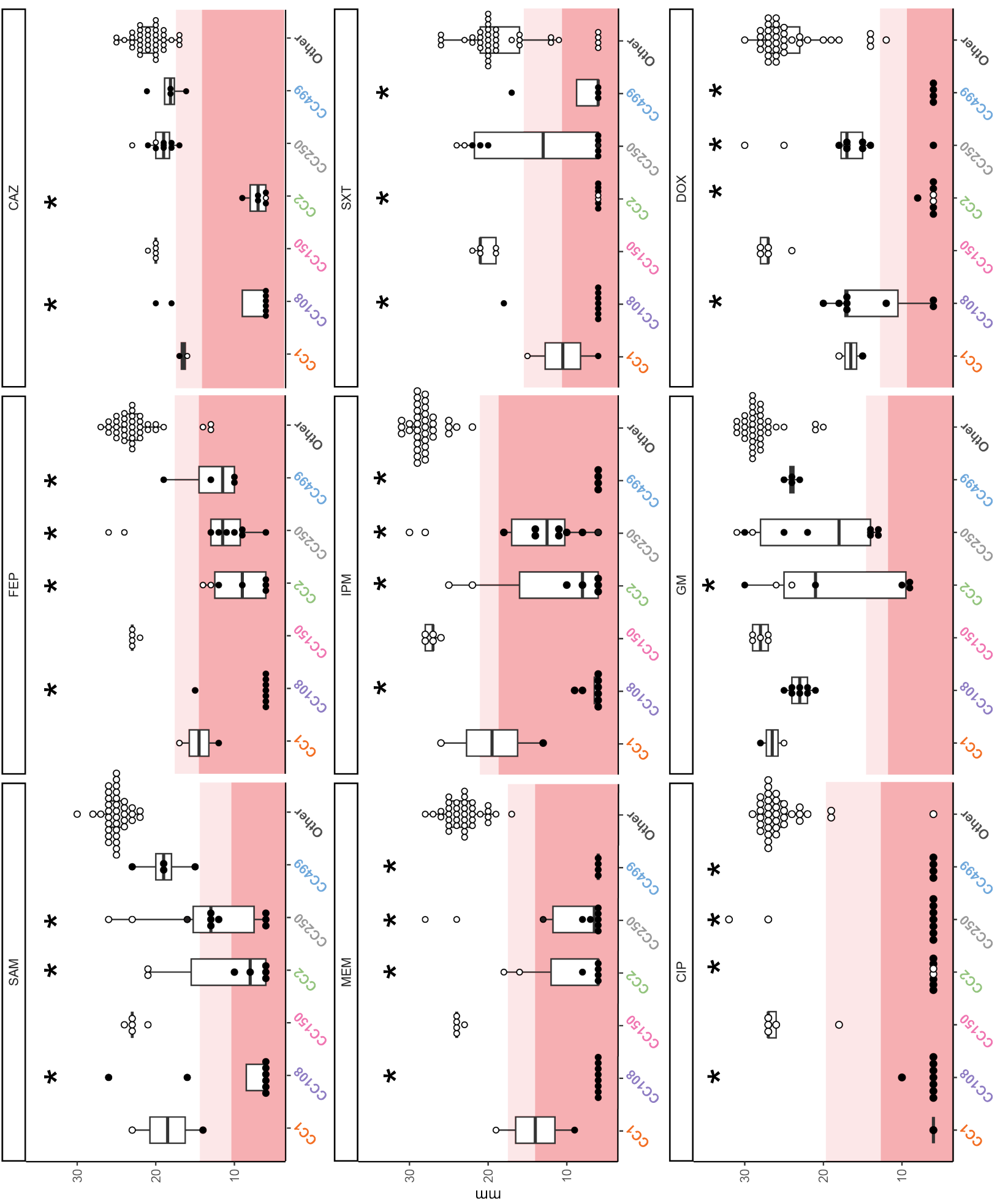








○ ●





### Isolate WU\_Ab164

